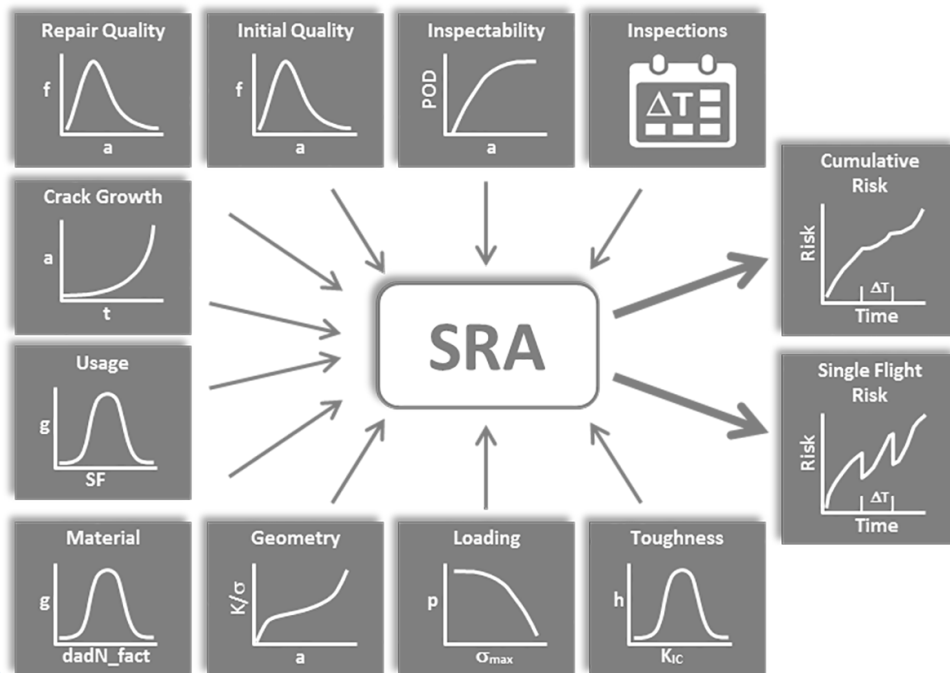


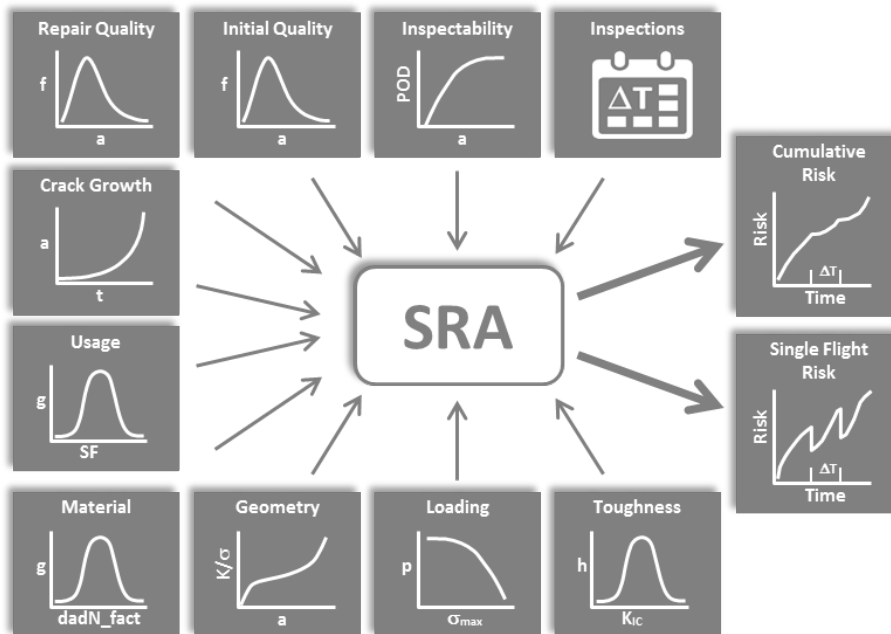


Probabilistic Fail-Safe structural risk analyses

CUSTOMER: Royal Netherlands Aerospace Centre



Probabilistic Fail-Safe structural risk analyses



REPORT NUMBER

NLR-TP-2020-416

AUTHOR(S)

F.P. Grooteman

REPORT CLASSIFICATION

UNCLASSIFIED

DATE

November 2020

KNOWLEDGE AREA(S)

Health Monitoring and Maintenance of Aircraft

DESCRIPTOR(S)

Fail-Safe
 Damage Tolerance
 Fatigue crack growth
 Probabilistic analysis
 Probability of failure

Problem area

Aircraft are designed according to the damage tolerance philosophy. Alternatively, a probabilistic damage tolerance analysis can be performed, called a structural risk analysis (SRA), taking into account all important scatter sources, such as, the initial flaw size, the inspection quality, the variability in loads and crack growth material properties. For new military aircraft, SRA is mandatory. For current aircraft, it already has become a valuable tool for fleet management, since it offers a risk (probability of failure) development over time, which cannot be obtained from the traditional deterministic damage tolerance analysis. It signals fleet management when to take corrective actions.

Description of work

This paper briefly describes SRA, which currently is applied to single load path structures only. Many aircraft structures however have multiple load paths, where after a (partial) failure of a load path the remaining structure can carry the limit load. Such a multiple load path structure can be analyzed by a so-call damage tolerance Fail-Safe analysis, which often results in a very conservative inspection scheme. The possibility that the crack can start in any of the load paths with a size that is much better represented by a distribution function than by some upper bound value, demands for a probabilistic approach. In this paper, a new probabilistic Fail-Safe approach is presented. The approach is an extension of the single load path SRA.

Results and conclusions

The new probabilistic Fail-Safe approach is demonstrated with a realistic example and compared against the deterministic Fail-Safe approach. The methodology has been implemented in the NLR in-house tool SLAP++. This tool also provides functionality to support the generation of the necessary structural risk analysis input.

GENERAL NOTE

This report is based on a presentation held at the Aircraft Structural Integrity Program (ASIP) conference, San Antonio, December 2019.

NLR

Anthony Fokkerweg 2

1059 CM Amsterdam, The Netherlands

p) +31 88 511 3113

e) info@nlr.nl i) www.nlr.nl



Dedicated to innovation in aerospace

NLR-TP-2020-416 | November 2020

Probabilistic Fail-Safe structural risk analyses

CUSTOMER: Royal Netherlands Aerospace Centre

AUTHOR(S):

F.P. Grooteman

NLR

This report is based on a presentation held at the Aircraft Structural Integrity Program (ASIP) conference, San Antonio, December 2019.

*The contents of this report may be cited on condition that full credit is given to NLR and the authors.
This publication has been refereed by the Advisory Committee AEROSPACE VEHICLES (AV).*

CUSTOMER	Netherlands Aerospace Centre
CONTRACT NUMBER	-----
OWNER	Netherlands Aerospace Centre
DIVISION NLR	Aerospace Vehicles
DISTRIBUTION	Unlimited
CLASSIFICATION OF TITLE	UNCLASSIFIED

APPROVED BY:		Date
AUTHOR	F.P. Grooteman	09-11-2020
REVIEWER	M.J. Bos	09-11-2020
MANAGING DEPARTMENT	M.J. Bos	09-11-2020

Summary

Many (aircraft) structures have multiple load paths where after a (partial) failure of a load path due to crack growth the remaining structure can carry the limit load without catastrophic failure or an overly severe impact on the operational characteristics of the whole structure, until the structure is repaired, replaced or modified. Such a multiple load path structure can be analyzed by a so-call Fail-Safe analysis. This however often results in a very conservative inspection scheme. Besides this, the possibility that the crack can start in any of the load paths with a size that is much better represented by a distribution function than by some upper bound value, demands a probabilistic approach.

In this paper a new probabilistic Fail-Safe approach is presented, in which the various uncertainties such as the initial flaw size, the inspection quality, the variability in loads and crack growth material properties, can be taken into account. The approach is an extension of the single load path structural risk assessment. The probabilistic approach is demonstrated with an example and compared against the deterministic Fail-Safe approach.

Contents

Abbreviations	5
1 Introduction	6
2 Deterministic Fail-Safe approach	10
3 Probabilistic Fail-Safe approach	12
4 Example	14
4.1 Problem definition	14
4.2 Deterministic Fail-Safe analysis	14
4.3 Probabilistic Fail-Safe analysis	15
4.4 Probabilistic Fail-Safe analysis load transfer sensitivity	17
5 Conclusions	19
6 References	20

Abbreviations

ACRONYM	DESCRIPTION
DTA	Damage Tolerance Analyses
EIFS	Equivalent Initial Flaw Size
FH	Flight Hour
POD	Probability Of Detection
POF	Probability Of Failure
SFPOF	Single Flight Probability Of Failure
SIF	Stress Intensity Factor
SLAP++	Stochastic Life Approach
SRA	Structural Risk Analysis
WFD	Widespread Fatigue Damage
a_{det}	Detectable crack size
a_{LT}	Crack size in the <i>primary</i> load path at load transfer
a_0	Initial flaw size
da/dT	Crack growth rate
T	Usage time
T_{fail1}	Time of failure of the <i>primary</i> load path
T_{FSLLI}	Fail-safety life limit for inspectable failures
T_{FSLLV}	<i>Fail-safety life limit</i> for visual evident failures
T_{LT}	Start time of load transfer
ΔT_{insp}	Inspection interval
	Superscript ^{<i>l</i>} and ^{<i>F</i>} denote an intact or failed primary load path
	Subscript ₁ and ₂ denote the <i>primary</i> and <i>secondary</i> load path

1 Introduction

It is well known that the service life of a structure loaded by an alternating load shows considerable variability (scatter) in crack growth life. This is mainly due to variability in manufacturing quality (i.e. initial crack size), load history and material properties. The current design philosophy applied for many structures is the so-called damage tolerance philosophy, formally introduced by the United States Air Force with the release of military standard MIL-A-83444 in July of 1974. It recognizes that a crack can develop during the service life of a structure and it assumes that cracks can already be present in the pristine structure at start of the service life. Safety is obtained from this approach by the requirements that either: 1) any crack be detected by routine inspection before it results in a dangerous reduction of the static strength (inspectable components), or 2) an initial crack shall not grow to a dangerous size during the service life (non-inspectable components).

Damage tolerance analyses (DTA) are basically deterministic, i.e. they do not consider the variability of the model parameters. Instead, they apply scatter factors and safety factors to the obtained crack growth life. In general, such analyses result in overly conservative life estimates and inspection intervals. Even so, the reliability (safety level, one minus the probability of failure) of the structure and its components is unknown. Moreover, the safety factors applied are quite arbitrary, although historically successful, possibly due to the high degree of conservatism.

Alternatively, a probabilistic damage tolerance analysis can be performed, further referred to in this paper as a structural risk analysis (SRA), in which the variability of all important scatter sources is taken into account in a probabilistic manner, see Figure 1. This requires the solution of a probabilistic problem and results in the quantification of the reliability level of the structure over time.

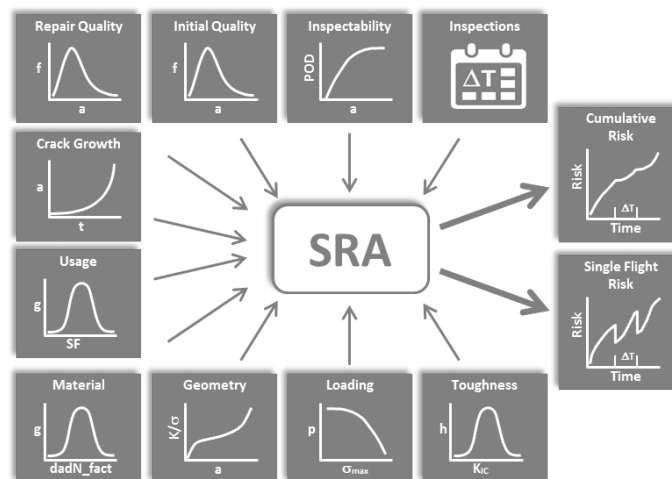


Figure 1: Structural risk analysis (SRA) overview

For new (military) aircraft SRA are prescribed in MIL-STD-1530D [1] and MIL-STD-882E [2]. In MIL-STD-1530D risk is defined in terms of the probability of failure to occur during the next flight (hazard rate) and in MIL-STD-882E in terms of the cumulative probability of failure (POF) during the life of the aircraft. Structural risk analyses have become a valuable tool for fleet management, since it offers a risk (probability of failure) development over time of the fleet and each individual aircraft which cannot be obtained from the traditional deterministic DTA. Figure 2 depicts a schematized structural risk analysis that starts from an equivalent initial flaw size distribution (EIFSD, indicated by 1) which develops over time (indicated by 2) and finally results in failures described by the failure distribution (indicated

by 3). Inspections, indicated by T_{insp} , can be performed to reduce the probability of failure by detecting most cracks before they result in a failure. As indicated in the figure, any inspection before T_{insp1} is useless, since cracks would be difficult to find with a reasonable chance of detection, determined by the probability of detection (POD, indicated by 4) curve of the applied inspection method.

The initial crack size in a damage tolerance analysis is based on pre-service inspection capability and is in general very conservative. This realization led to the concept of equivalent initial flaw size (EIFS) [3]. EIFS values are a substitute for any real (and unknown) initial damage in the structure at start of service life. An issue is that an EIFS is derived by back-calculation from actual detectable long cracks, using macro-crack growth models. These models are in general unable to describe the real behavior of cracks that grow from any (very small) initial damage at start of service life. The resulting EIFS distribution at start of service life, depicted in Figure 2 on the y-axis, is therefore often unrealistic, because the crack growth rate is ill-predicted by the macro-crack growth models for the main part of the lifetime. Only in special cases, such as the exponential crack growth that is often seen for military aircraft spectra [4], back-calculation may result in a realistic initial flaw size.

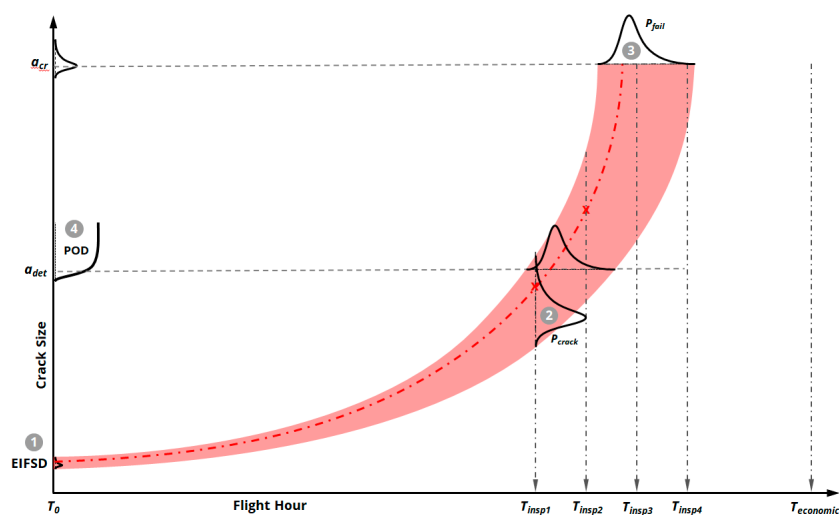


Figure 2: Schematized structural risk analysis

Instead of using EIFS to predict crack growth from the start of service, an alternative [5] is to start the analysis from the failure distribution at the end of service life (indicated by 3). Backward crack growth analyses are performed only down to the detectable crack size, where a large crack growth model still is applicable. One of the main advantages of such an approach is that during service the calculated failure distribution, unlike the EIFS distribution, can be validated and updated using inspection data. The EIFS distribution in general cannot be validated since it does not represent real crack sizes.

Both approaches to compute the risk level over time, starting from an EIFS or failure distribution, have been implemented in a C++ computer code called SLAP++ (Stochastic Life Approach) [6], which is based on object oriented principles. SLAP++ is a dedicated probabilistic tool to perform structural risk analyses for individual aircraft and a fleet of aircraft. The input of the tool, shown in Table 1, is based on the data gathered during the execution of the Aircraft Structural Integrity Program (ASIP) of which some are required and the remainder is optional. The table also indicates whether the risk is sensitive for the input. The Monte-Carlo simulation (MCS) method is applied to compute the failure probability. In each simulation an initial flaw size is drawn from the EIFSD and from the crack growth curve the failure time can be determined, as well as the crack sizes at the inspection times. In case of load and/or material variability, a scaled crack growth curve is applied. For each inspection, the probability value obtained from the POD for the given

crack size is compared with a random drawn probability value, and the crack is detected when this value is smaller than the POD value. A failure occurs, if the crack is not detected at all inspections and the failure time is less than the economic life.

The structural geometry in which the crack is located strongly determines the stress distribution at the crack tip, represented by the stress intensity factor (SIF). Together with the material properties and applied load sequence, which both can show significant variability with a high impact on the risk levels, this determines the crack growth curve. The critical crack size is the last point of the crack growth curve. Failure may occur at different critical crack sizes depending on the applied maximum stress in the load cycle at failure, the variability in fracture toughness value and the stress intensity solution specified by the crack geometry. Therefore, if the user has specified a maximum stress distribution, a fracture toughness distribution and crack geometry, this input will be used to compute the critical crack size. Otherwise, the maximum crack size from the crack growth curve will be applied. In general, the crack growth curve will be (very) steep close to failure (a small change in life corresponds to a large change in crack size) and therefore the structural risk analysis results will not be sensitive for variability in critical crack size. Hence, all of the related inputs are optional. If no repair distribution is specified it is assumed that, in case of crack detection, the component is replaced with a redesigned version not having the failure mode. Some other characteristics of the tool are:

- It can take into account load severity and scatter in material crack growth properties that can have a significant effect on the structural risk.
- It can start from the failure distribution instead of the equivalent initial flaw size distribution, of which only the failure distribution can be validated.
- It does not put any restrictions on the selected distribution functions.
- It comes with data analysis tools to characterize the distribution functions.
- It uses MCS instead of direct integration to solve the probabilistic problem yielding a result that always converges to the exacted solution.
- It computes the true hazard rate instead of the approximated single flight probability of failure (SFPOF).
- It can automatically determine an optimal inspection scheme.
- It can combine individual risk plots of multiple components.
- It comes with a GUI.

Table 1: SLAP++ input

Data Category		Description	Sensitivity
Aircraft/Usage			
Crack growth curve	required	Crack growth curve from DTA	High
Initial flaw size	required	Initial crack size distribution	High
Maximum stress	optional	Maximum stress per flight distribution	Low
Load severity	optional	Crack Severity Index distribution	High
Material scatter	optional	Scale Factor distribution	High
Hours per flight	optional	Average flight length	Low
Material/Geometry			
Crack geometry	optional	Stress Intensity Factor curve from DTA	Low
Fracture toughness	optional	Fracture toughness distribution	Low
# of locations	required	Number of similar locations in one airframe	Moderate
Inspection/Repair			
Inspection scheme	optional	Inspection times or maximum hazard rate	High
Probability of detection	required	Probability of detection distribution of NDI system capability	Moderate
Repair quality	optional	Repair crack size quality distribution	Low

An example of the resulting hazard and cumulative failure probability plot, specifying the risk level over time, are shown in Figure 3, for an increasing number of inspections. The hazard rate (left plot) will start to increase from the start of the usage interval. At some point in time, when the first cracks become large enough to cause failures, the hazard rate will reach values visible in the hazard plot. In the example, this is the case around 4500 FH. Without inspections the hazard rate will increase to very high levels. At 5200 FH an inspection is applied and many large cracks will be found and no longer cause failure. Hence, the hazard rate will drop at the inspection, but after a while will rise again when smaller cracks have grown to critical crack sizes. This causes the characteristic discontinuities in the hazard plot at the 4 inspections. After even the smallest initial cracks, from the lower tail of the EIFSD, have grown to failures or are detected, no large cracks and therefore failures are present anymore. The hazard rate then drops to zero again, as can be seen around 6800 FH in the left plot.

The cumulative failure on the other hand is an increasing function by definition and only the rate of increase slows down at an inspection, causing the characteristic dips in the cumulative curve as can be seen in the right plot of Figure 3. When no failures occur anymore, the cumulative curve remains constant. The noise visible in the bottom area of the plots at the very small probability values can be removed by increasing the number of simulations, requiring additional computational effort not gaining any significant improvement in accuracy.

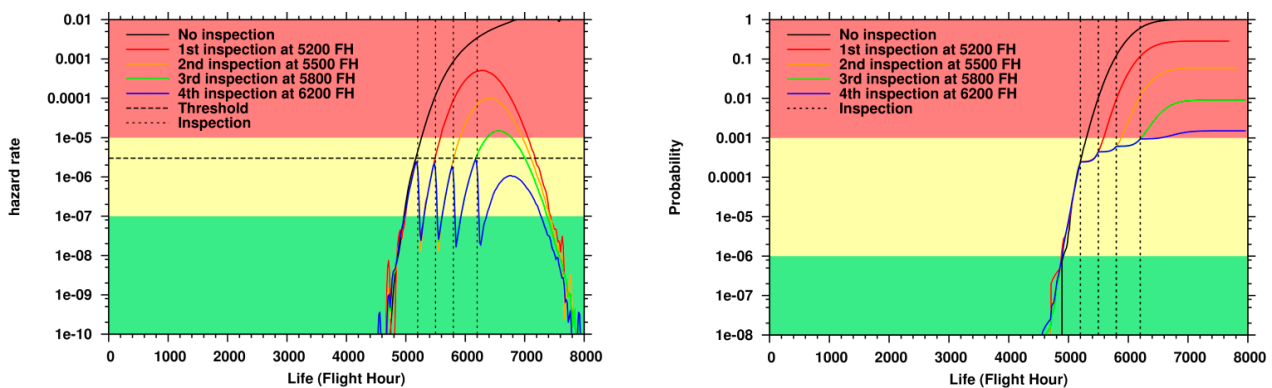


Figure 3: SLAP++ hazard rate (left) and cumulative risk (right) plots for an increasing number of inspections

The colors in the hazard and cumulative probability of failure plot represent the threshold risk levels as indicated in MIL-STD-1530D and MIL-STD-882E for a catastrophic failure and indicate a *safe/adequate* situation (green bottom region), a risk level that is regarded *undesirable* (yellow middle region) and a risk level that is regarded *unacceptable* (red top region). When the risk becomes undesirable risk mitigation should be applied, for instance by inspection, repair, replacement, modification or operational restrictions. In the example above, the hazard rate remains in the yellow region throughout the four inspections. The cumulative risk still is undesirably high after 6200 FH.

The above SRA is for a single load path structure. Recently, the SLAP++ tool has been extended with the unique capability to perform a structural risk analysis for multiple redundant load path structures, i.e. a probabilistic Fail-Safe analysis. A general description of the deterministic Fail-Safe approach is provided in section 2. Section 3 details the probabilistic Fail-Safe approach and an example is discussed in section 4.

2 Deterministic Fail-Safe approach

Many (aircraft) structures have multiple load paths where after a (partial) failure of a load path the remaining structure can carry the limit load without catastrophic failure or an overly severe impact on the operational characteristics of the whole structure, until the structure is repaired, replaced or modified. The (partial) failure shall be either readily detectable by *visual* inspections or through a malfunction event, for instance fuel leakage or loss of cabin pressure. However, also NDI inspections can be performed to detect any problem long before an expensive (partial) load path failure or in cases where a visual inspection cannot be performed. This is captured by a deterministic Fail-Safe analysis that has always been part of the damage tolerance methodology, although the main focus has been on the single load path slow crack growth concept. An excellent reference of the deterministic Fail-Safe concept is provided in the structure bulletins by DeFasio [7].

The shortcomings of the deterministic single load path slow crack growth concept are that it doesn't address the issues of continuing damage in the adjacent structure, safe periods of unrepaired usage after a load path failure and the fact that the fail-safety will be jeopardized later in life by the onset of widespread fatigue damage (WFD) [7]. Moreover, there is no operational life limit of the structure, but the aircraft structure is thought to be retired when the economic burden or aircraft down times associated with all of the inspections and repairs will become too high. However, this nowadays is questioned since this is only true when all inspections are correctly performed and depots have enough resources to handle the increased inspection and repair burden for aging aircraft. This makes the Fail-Safe design the preferred concept since it provides large damage capability and is the only concept that protects against all forms of damage an aircraft may encounter during its lifetime, including fatigue cracking, corrosion, accidental damage, manufacturing defects, manufacturing or maintenance induced damage, and even discrete source damage such as engine burst, bird strike, hail, battle damage [7]. Due to this, the Fail-Safe concept has drawn more and more attention, also for existing aircraft not initially designed as such but having many multiple load path structures with inherent Fail-Safe capability [7]. For instance, the wing structure of a fighter plane, consisting of multiple spars and a lower and upper skin, schematically depicted in Figure 4, often can sustain a broken spar. A broken spar may lead to a large crack in the wing skin that can easily be detected by visual inspection or may result in fuel leakage. Other examples are a vertical stabilizer and wing attach fittings or a wing carry through bulkhead.

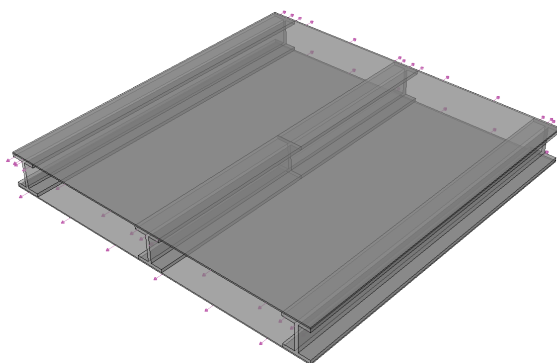


Figure 4: Stiffened skin with broken spar

The deterministic Fail-Safe approach is schematized in Figure 5, depicting the crack growth curve of the *primary* load path (red dashed-dot curve) and the *secondary* load path for an *intact* (solid curve) and for a *failed* (dashed curve) primary load path. The latter crack growth curve is with fully redistributed loads at $T=0$, assuming primary load path failure at start of the usage interval, showing accelerated crack growth and a smaller critical crack size (a_{cr2F}) at failure.

This results in a *safe period of unrepaired usage* (T_{SPUU}), being the time for initial flaws in the *secondary* structure to reach their critical size under the redistributed limit loads. These initial flaws can be due to manufacturing and/or material defects like hole drilling defects, weld defects and inclusions. Both *secondary* load path crack growth curves start with the same initial crack size a_0 representative of normal material and manufacturing quality. The assumed initial crack size is a 0.254 mm (0.01 inch) corner crack at the most critical (fastener) holes and cut-outs or a 0.254 mm (0.01 inch) deep by 0.508 mm (0.03 inch) long surface crack at other critical locations unless data exists to justify another assumption [7].

The projection of the critical crack size for the *secondary* load path with *failed* primary load path a_{cr2F} on the curve for the *secondary* load path with the *intact* primary load path defines the *fail-safety life limit* for visual evident failures (T_{FSLLV}). Beyond this point, there is an increased probability that if there was a failure of the *primary* load path, the adjacent structure would not have sufficient residual strength to prevent loss of the aircraft and the structure would no longer be Fail-Safe. If failure of the *primary* load path is not immediately obvious a scheduled (visual) inspection is required. For a given inspection interval, depicted in the figure as ΔT_{insp} , and assuming the *primary* structure failed just after the last inspection, the reduced fail-safety life limit for inspectable failures (T_{FSLLI}) can be found by projecting an assumed existing crack size. Vice versa for a given fail-safety life limit for inspectable structures T_{FSLLI} the corresponding inspection interval ΔT_{insp} can be obtained.

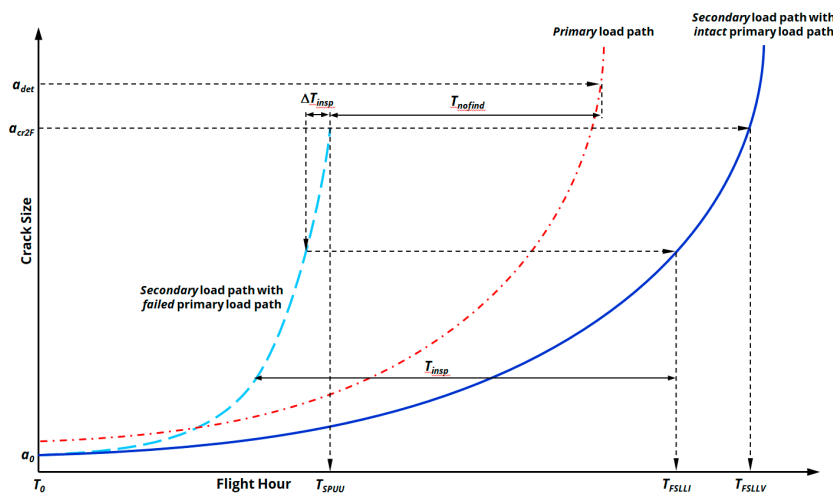


Figure 5: Schematized deterministic Fail-Safe approach

As depicted in Figure 5 by T_{insp} , inspections every ΔT_{insp} start halfway the safe period of unrepaired usage T_{SPUU} for which it has been assumed that the *primary* load path already failed at the start of the usage interval. This is extremely conservative and will result in many unnecessary inspections with no finds as will be demonstrated in section 4 for the probabilistic analysis. In the case of visual inspections the detectable crack size (denoted a_{det} in Figure 5) will be large and cracks will most likely only become detectable near the end of the usage life. In the case of a simple visual inspection this inspection burden may be acceptable. However, as stated above NDI techniques may be applied as well in order to find cracks long before an expensive failure of the *primary* load path or in cases where a simple visual inspection does not apply. The latter, for instance is true for many locations where a large crack is not visible on the outside and disassembly of other structural parts is required, making the inspection time consuming and more costly, e.g. vertical stabilizer attach fitting. A broken wing spar for example, only becomes visible once the skin has significantly cracked as well (possibly resulting in fuel leakage which makes detection even easier). If the crack has to be detected at an earlier stage, an NDI method, for instance an expensive CT scan in the case of a wing structure, has to be applied and the number of inspections should be minimized.

3 Probabilistic Fail-Safe approach

Besides the very conservative number of inspections resulting from a deterministic Fail-Safe analysis, the possibility that the crack can start in any of the load paths with a size that is much better represented by a probabilistic distribution function (EIFS distribution) than by an upper bound value (rogue flaw), demands a probabilistic approach. This is schematically demonstrated in Figure 6. The initial crack size in both the *primary* and *secondary* load path is defined by an EIFSD. This not necessarily has to be the same EIFS distribution for both load paths, it can for instance differ for a spar and a skin, denoted in the figure by EIFSD₁ and EIFSD₂. Both EIFS distributions cause a variation in possible crack growth curves, depicted by the colored areas, where curves near the lower and upper tail of the EIFS distributions are less likely to occur. Note, that the same crack growth curves of the deterministic Fail-Safe analysis of Figure 5 are included in the probabilistic Fail-Safe figure as well, indicating one of the possible combinations that can occur. The crack detectability is represented by the probability of detection (POD) curve as shown on the left, giving the chance to detect a crack of a certain size, which for visual inspections is in the high crack size range, but may be shifted downwards for an NDI method. The area where cracks in the *primary* load path become detectable in size and time is depicted in the figure by the square grey area. Hence, it makes no sense to start inspecting well before T_{insp1} or after T_{insp3} as indicated in the figure. Any cracks at for instance T_{insp0} will be way too small to be detected by the indicated visual inspection method.

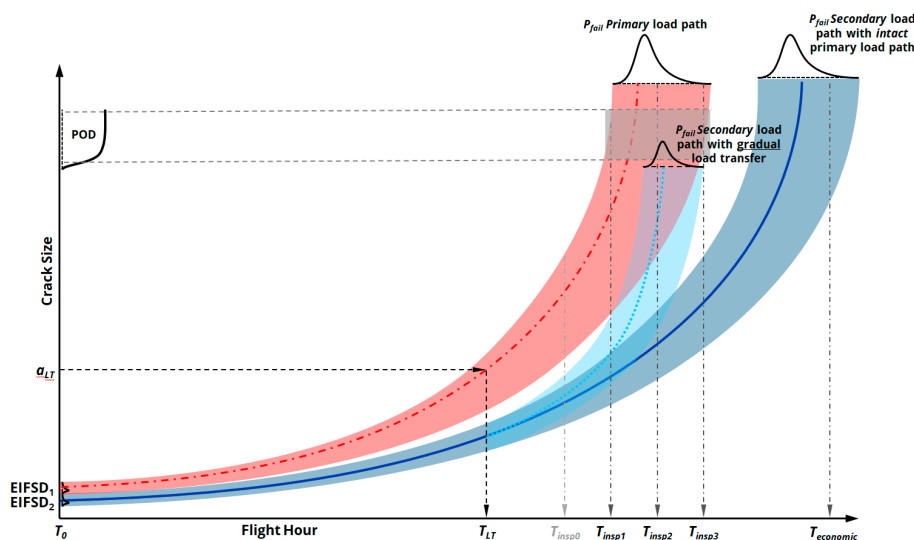


Figure 6: Schematized probabilistic Fail-Safe analysis

Another important difference between the deterministic and the probabilistic approach is the derivation of the inspection times. As shown in Figure 5 the inspection interval ΔT_{insp} is selected in the deterministic approach and starts before T_{SPUU} . In the probabilistic approach the inspection times are determined from the risk level in terms of the hazard rate or cumulative probability of failure. Only when the risk exceeds a prescribed threshold an inspection is performed, detecting larger cracks and lowering the risk. In this way an optimal inspection scheme can be derived minimizing the number of inspections. This is demonstrated in section 4.3.

The (dark-blue) area in Figure 6 around the solid curve denotes the variation in crack growth curves for the secondary load path with *intact* primary load path. From a certain crack size a_{LT} in the *primary* load path, load redistribution to the *secondary* load path will take place, altering these crack growth curves, as depicted by the (light-blue) area around the dotted curve. This is not taken into account in the deterministic Fail-Safe approach, which considers only the

secondary load path crack growth curve with full load transfer after a failed primary load path right at the start of the usage period ($T=0$). The value of the crack size a_{LT} can be set by the user and by default is half the critical crack size of the primary load path. In section 4.4 the effect of this choice will be demonstrated. Apart from this, two different options are implemented to address the load transfer; they are schematically depicted in Figure 7. In the first option, full load transfer is assumed at T_{LT} , similar as in the deterministic analysis, and the crack growth curve of the *secondary* load path with *intact* primary load path switches to the crack growth curve with *failed* primary load path, which is conservative. In the second option, a gradual (more realistic) load transfer is applied from the start of load transfer T_{LT} up to the time of failure of the *primary* load path T_{fail1} , where the crack growth rate da/dT at each crack size a_i is a linear interpolation of the crack growth rates of the *secondary* load path crack growth curves with intact and failed primary load path, as indicated in Figure 7.

$$\frac{da}{dT_i} = \frac{\left(\frac{da^F}{dT_i} - \frac{da^I}{dT_i}\right)T_i + \left(T_{fail1} \frac{da^I}{dT_i} - T_{LT} \frac{da^F}{dT_i}\right)}{T_{fail1} - T_{LT}} \quad (1)$$

in which the superscript I and F denote the *secondary* crack growth curve with intact or failed primary load path. At T_{LT} , the crack growth rate for the crack size a_i is equal to the intact curve and at *primary* load path failure T_{fail1} to the failed curve. After T_{fail1} the remainder of the crack growth curve of the *secondary* load path with failed primary load path is applied. The computation of the crack growth curve for the gradual load transfer according to equation (1) takes more computational effort. Because this has to be done for each probabilistic simulation, the total analysis time for the second method is significantly (approximately a factor 5) higher than for the first method. In section 4.4 the effect of both options on the risk level will be shown.

Apart from the additional crack growth curves (four in total) and EIFSD distribution, the input for a probabilistic Fail-Safe analysis is the same as for a single load path SRA.

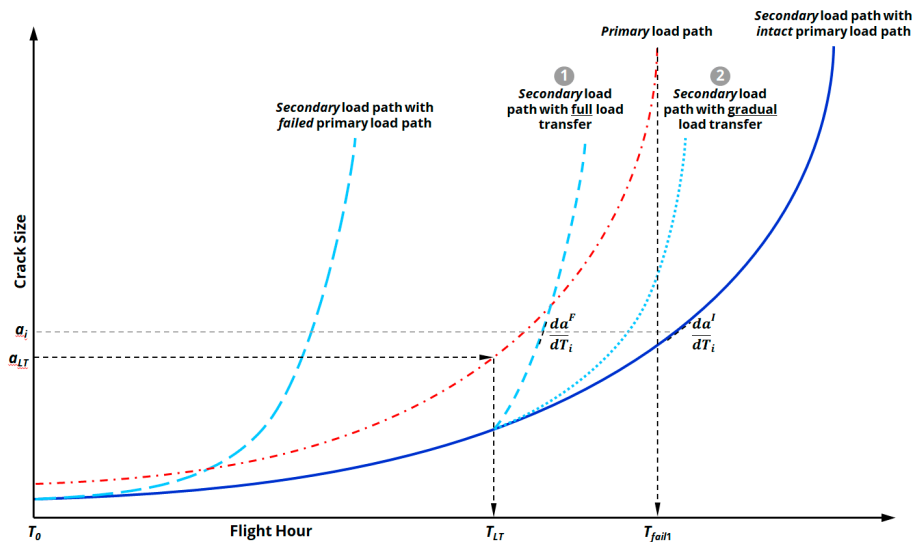


Figure 7: Secondary crack growth curves, assuming full (1) or gradual (2) load transfer at T_{LT}

4 Example

4.1 Problem definition

A structure will often have a somewhat different geometry and loading for each load path and therefore somewhat different crack growth curves. For instance, a wing structure with differences in geometry and load transfer in each spar. Figure 8 depicts the four crack growth curves that can be considered as the crack growth curves for two different wing spars. They can be determined from a crack growth analysis or from experimental data. For each load path, two curves need to be successively specified, for the intact and failed counter load path. Here, it is assumed that the crack growth shows exponential behavior according to equation (2), i.e. straight lines on a log-scale, which is common for fighter aircraft spectra [4], using the following β values: 0.9, 1.3, 0.94 and 1.4.

$$a = a_0 e^{\beta T} \quad (2)$$

The initial flaw size a_0 of 0.001 mm has been selected to be far in the lower tail of the EIFS distribution that is provided in Figure 10.

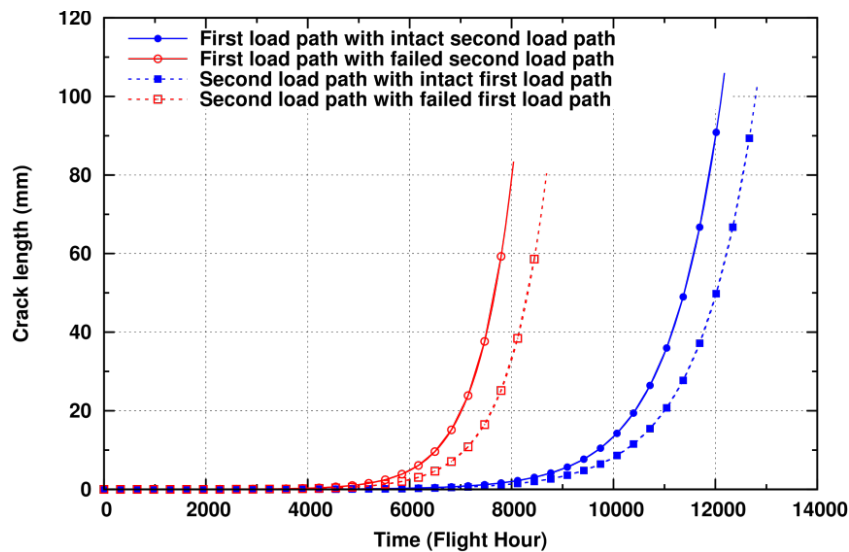


Figure 8: Crack growth curves for the first (solid lines) and second (dashed lines) load path with intact (solid symbols) or failed (open symbols) counter load path

4.2 Deterministic Fail-Safe analysis

The deterministic Fail-Safe analysis for the most critical first load path, with initial flaw size of 0.254 mm (0.1 inch), is depicted in Figure 9 for a 200 flight hour (FH) inspection interval. Based on the 200 FH inspection interval, the fail-safety life limit of 5810 FH is determined as indicated by the arrows. As applied by OEMs, the inspections start at half the safe period of unrepaired usage 2072 FH ($0.5 \cdot 4144$), requiring a total of 19 ($\text{floor}(5810-2072)/200+1$) inspections up to the fail-safety life limit. A larger inspection interval can be selected but yields a lower T_{FSL} .

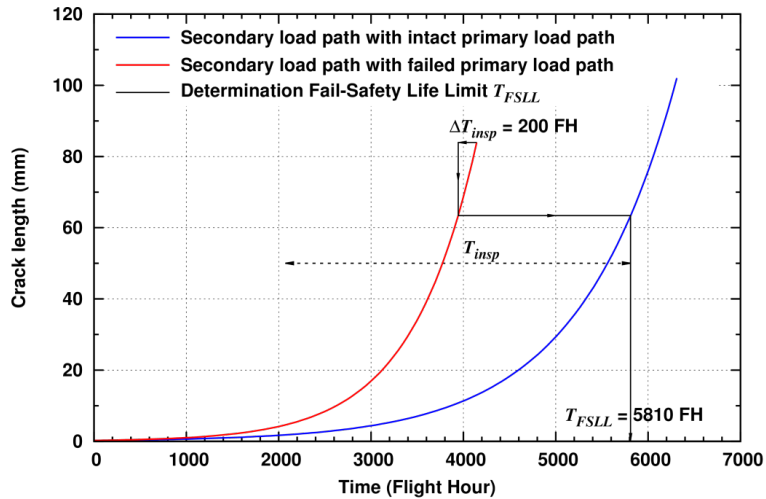


Figure 9: Deterministic Fail-Safe analysis for a 200 FH inspection interval

4.3 Probabilistic Fail-Safe analysis

In [8], over 560 initial flaw sizes and their corresponding discontinuity depth data from various types of surface discontinuities (etched pit, peening, damage and inclusions) were examined for 7050 aluminum alloy, and the largest median was found to result from mechanical damage in hole bores which may be the most critical in the absence of other discontinuities, having a lognormal(-3.72, 0.955) initial flaw size distribution, depicted in Figure 10. The initial flaw size a_0 of 0.254 mm, as applied in the deterministic analysis, is also depicted, far in the upper tail by the solid circle. The probability of occurrence of a crack with a size equal to or greater than a_0 is $7E-3$. Exponential crack growth was observed up to very small crack sizes [4] and the EIFSD can be regarded as an IFSD. If threshold behavior at small crack sizes is present, however, this easily can be modelled by a lower bound on the (E)IFSD. For both load paths the same (E)IFSD is selected since the manufacturing and material properties are assumed to be the same for all spars. The (E)IFSDs for the two load paths are not correlated, however SLAP++ does provide the option to apply a correlation between random variables. Depending on the initial crack size and corresponding failure time of each load path, the first one that fails is the *primary* load path, which can differ between the different simulations. Therefore, in Figure 8 the two load paths are denoted as first (solid curves) and second (dashed curves), which thus does not correspond to primary and secondary!

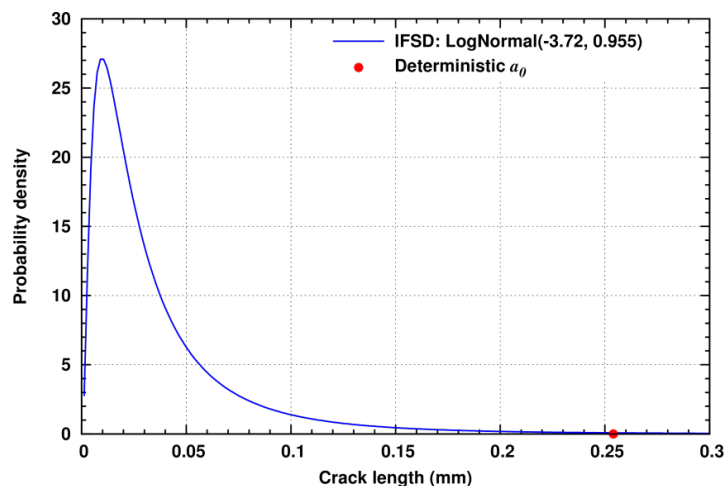


Figure 10: Initial flaw size distribution as applied for both load paths

The hazard rate plot without inspections is shown in Figure 12 (open circle symbols) and around 6800 FH the level becomes unacceptably high. The plot also shows that before the deterministic fail safety life limit of 5810 FH (dashed-dotted line in Figure 12), the hazard rate is very low and still close to the lower adequate region. This means that all 19 inspections obtained in the deterministic Fail-Safe analysis are redundant and do not result in many crack findings, which was confirmed by a probabilistic analysis. This demonstrates the huge level of conservatism of the deterministic Fail-Safe analysis, mainly caused by assuming a failed *primary* load path at start of the usage interval and a conservative upper bound of the initial flaw size.¹

Inspections can decrease the risk level by detecting and repairing/replacing cracks before they result in a failure. The assumed POD curve, lognormal(3, 0.7) depicted in Figure 11 (blue solid line), has a minimum detectable crack size of 10 mm and only large cracks can be found reliably. This represents a visual inspection or a crack in a spar that can only be found by means of an NDI method, for instance a CT scan of the wing. Figure 12 shows the automatically determined optimal inspection scheme [6222, 6854, 7359, 7832] FH for a maximum allowed hazard rate of 1.E-6 (solid blue line). Only four inspections, instead of 19 for the deterministic analysis, are required that even start after the deterministic fail safety life limit T_{FSL} . Moreover, with the four inspections the hazard rate stays well below the unacceptable upper region up to the economic life of 8000 FH instead of the fail safety life limit of 5810 FH.

To demonstrate the influence of the POD curve on the hazard rate, an additional analysis is presented having a POD that can only detect even larger cracks reliably, depicted in Figure 11 by the orange round symbols. Figure 12 also shows the hazard rate plots obtained for this second POD. The orange POD requires ten inspections at [6222, 6599, 6812, 7025, 7195, 7351, 7492, 7624, 7756, 7871] FH, instead of four, to keep the hazard rate below the threshold level.

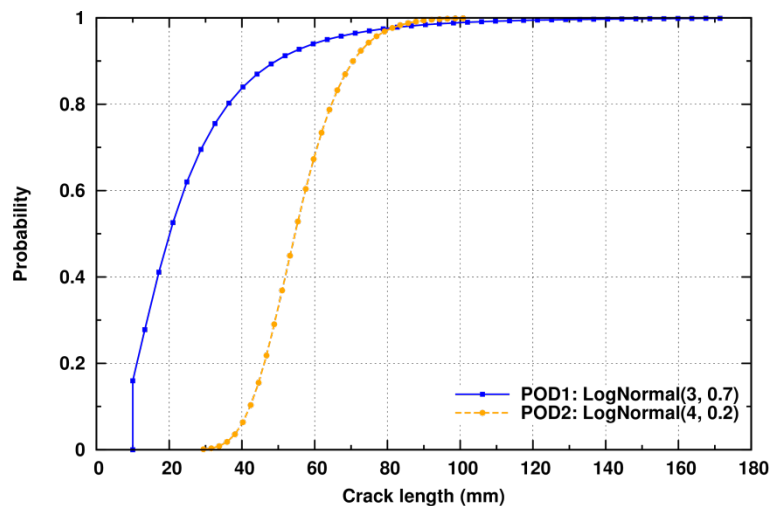


Figure 11: Probability of Detection curve with minimum detectable crack size of 10 mm

¹ It is noted that the deterministic fail safety damage tolerance approach also provides safety in case of discrete source damage such as engine burst, bird strike, hail and battle damage; these types of damage may occur at any moment in the life of an aircraft. It is also noted, however, that in most cases these types of damage are obvious and do not require directed inspections.

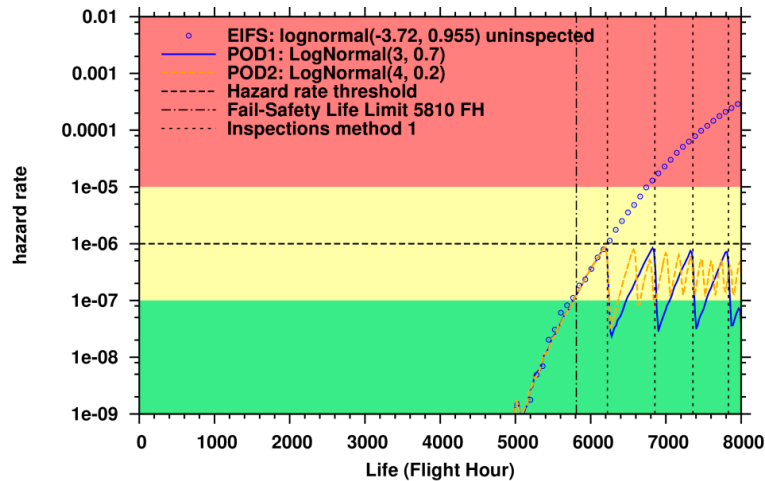


Figure 12: Hazard rate plot without and with optimal inspections for a 1.E-6 threshold for different PODs

4.4 Probabilistic Fail-Safe analysis load transfer sensitivity

As explained in section 3 for the probabilistic Fail-Safe approach, the start of load transfer from the *primary* to the *secondary* load path is defined as a percentage of the critical crack size. Furthermore, two methods are available to construct the crack growth curve of the *secondary* load path with load transfer, assuming full load transfer or a much more realistic gradual load transfer. Figure 13 shows the hazard rate without inspections for both load transfer methods and different values of the percentage critical crack size in the *primary* load path at start of load transfer. The red (plus and closed) symbols represent the gradual load transfer of method 2. For both methods the hazard rate curves are similar but are shifted to the right for an increasing percentage. For 0%, load transfer starts right from the start of the usage interval. For method 1, this is similar as assumed in the deterministic Fail-Safe approach and results in a very conservative hazard rate already becoming unacceptably high around 4800 FH. Assuming that load transfer starts at a more realistic higher percentage of the critical crack size of the *primary* load path a_{cr1} , rapidly shifts the curves to the right. At 25% a_{cr1} the hazard curve for both methods already is close to the 75% curves and there is not much difference between a 50% or 75% value, which is even less for the more exact method 2. In general, one might expect that at 25% a_{cr1} load transfer is (very) small. Hence, for method 2, yielding the much more realistic crack growth curve, this can be regarded as a conservative default value. The corresponding hazard rate curve (solid-square symbols) more or less coincides with the 50% a_{cr1} value for method 1 (open-circle symbols) with the (much) higher crack growth, also depicted in Figure 14.

Figure 14 also shows the hazard rate with optimal inspections for a threshold hazard rate level of 1.E-6 computed for method 1 with a 50% and method 2 with a 25% a_{cr1} value. As for the uninspected hazard rate plot, both curves show a comparable result. The inspection scheme obtained for method 2 [6181, 6804, 7301, 7752] FH is comparable to the one obtained for method 1 [6222, 6854, 7359, 7832] FH. Hence, by default the load transfer, which can be adjusted by the user, is modelled with the faster and conservative method 1 (full load transfer) and is assumed to start when the crack in the *primary* load path has reached half the critical crack size (50% a_{cr1}).

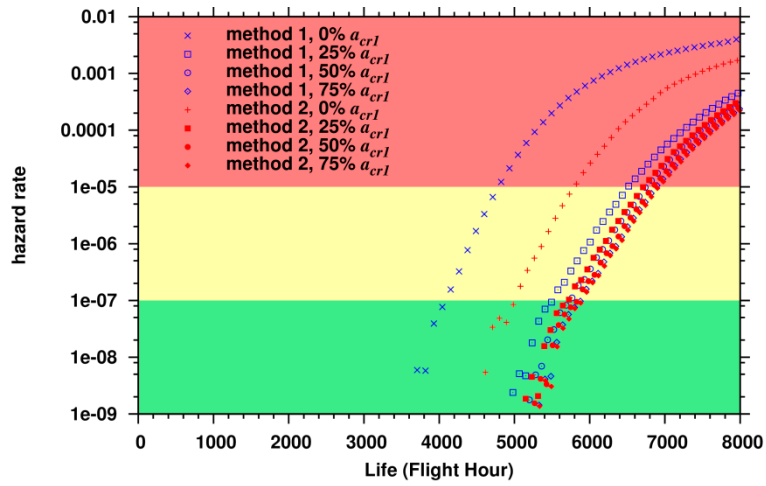


Figure 13: Hazard rate plot without inspection for different critical crack percentage values

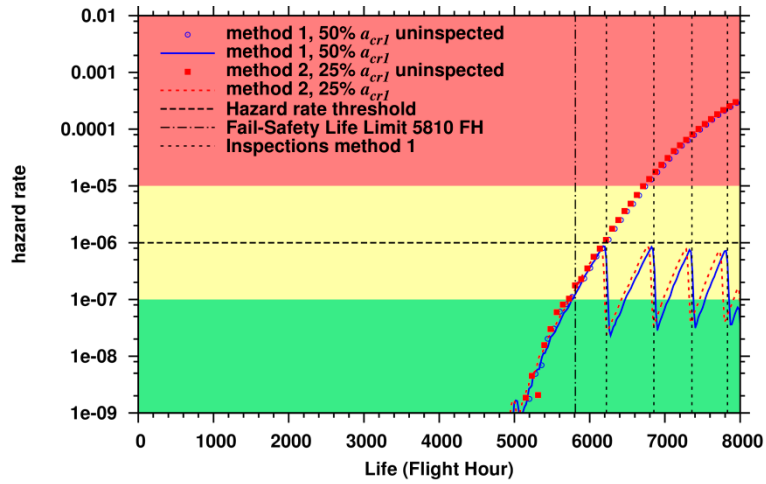


Figure 14: Hazard rate plot without inspection for different crack percentage values

5 Conclusions

A probabilistic Fail-Safe approach was presented, in which the various uncertainties such as the initial flaw size, the inspection quality, the variability in loads and crack growth material properties, can be taken into account. The approach is an extension of the single load path structural risk analysis. The probabilistic approach was demonstrated with an example and compared against the deterministic Fail-Safe approach, demonstrating the high level of conservatism of the deterministic Fail-Safe method, yielding mostly redundant inspections. By application of a probabilistic Fail-Safe analysis, the costs of inspections and down-time can tremendously be reduced together with an increase in the life time of the structure, especially when an NDI technique is applied in order to find cracks long before an expensive failure of the primary load path or in cases where a simple visual inspection does not apply.

The sensitivity of the probability of detection distribution and choice of load transfer method on the hazard rate curve was also demonstrated. From the latter good default values for the load transfer method were derived.

6 References

1. MIL-STD-1530Dc1, Department of Defense Standard Practice for ASIP, 13 October 2016.
2. MIL-STD-882E, Department of Defense Standard Practice for System Safety, 10 May 2012.
3. S.D. Manning, J.N. Yang, USAF Durability Design Handbook, AFFDL-TR-84-3027, Air Flight Laboratory, Wright Patterson AFB, 1984.
4. L. Molent a, M. McDonald, S. Barter, R. Jones, Evaluation of spectrum fatigue crack growth using variable amplitude data, *Int J Fatigue* 30 (2008) 119–137.
5. F.P. Grooteman, A stochastic approach to determine lifetimes and inspection schemes for aircraft components, *Int J Fatigue*, 30 (2008) 138–149.
6. F.P. Grooteman, Stochastic Life Approach: SLAP++ User Manual v3.0, NLR-TR-2017-022, 2019.
7. M. DeFazio, H. Yeh, Structures Bulletins EN-SB-08-001/003 on Fail-Safe structures, ASC/EN, 2008.
8. <http://www.saf-engineering.com/images/EN-SB-08-001.pdf>.
9. L. Molent, A review of equivalent pre-crack sizes in aluminium alloy 7050-T7451, *Fatigue Fract Engng Mater Struct* 37 (2014) 1055-1074.



Dedicated to innovation in aerospace

NLR - Royal Netherlands Aerospace Centre

Royal NLR operates as an unaffiliated research centre, working with its partners towards a better world tomorrow. As part of that, Royal NLR offers innovative solutions and technical expertise, creating a strong competitive position for the commercial sector.

Royal NLR has been a centre of expertise for over a century now, with a deep-seated desire to keep innovating. It is an organisation that works to achieve sustainable, safe, efficient and effective aerospace operations.

The combination of in-depth insights into customers' needs, multidisciplinary expertise and state-of-the-art research facilities makes rapid innovation possible. Both domestically and abroad, Royal NLR plays a pivotal role between science, the commercial sector and governmental authorities, bridging the gap between fundamental research and practical applications. Additionally, Royal NLR is one of the large technological institutes (GTIs) that have been collaborating since 2010 in the Netherlands on applied research as part of the TO2 federation.

From its main offices in Amsterdam and Marknesse plus two satellite offices, Royal NLR helps to create a safe and sustainable society. It works with partners on numerous (defence) programmes, including work on complex composite structures for commercial aircraft and on goal-oriented use of the F-35 fighter. Additionally, Royal NLR helps to achieve both Dutch and European goals and climate objectives in line with the Luchtvaartnota (Aviation Policy Document), the European Green Deal and Flightpath 2050, and by participating in programs such as Clean Sky and SESAR.

For more information visit: www.nlr.org

Postal address

PO Box 90502
1006 BM Amsterdam, The Netherlands
e) info@nlr.nl i) www.nlr.org

NLR Amsterdam

Anthony Fokkerweg 2
1059 CM Amsterdam, The Netherlands
p) +31 88 511 3113

NLR Marknesse

Voorsterweg 31
8316 PR Marknesse, The Netherlands
p) +31 88 511 4444